

## Barrier distributions from $^{32}\text{S}+^{90,96}\text{Zr}$ quasi-elastic scattering: Investigation of the role of neutron transfer in sub-barrier fusion reactions

F. Yang,\* C. J. Lin, X. K. Wu, H. Q. Zhang, C. L. Zhang, P. Zhou, and Z. H. Liu  
*China Institute of Atomic Energy, P. O. Box 275, Beijing 102413, People's Republic of China*  
 (Received 19 September 2007; published 4 January 2008)

The differential cross sections of quasi-elastic scattering at backward angles were measured with high precision for  $^{32}\text{S}+^{90,96}\text{Zr}$  around the Coulomb barrier, and barrier distributions were extracted from the measured excitation functions. The experimental barrier distribution of  $^{32}\text{S}+^{90}\text{Zr}$  is well reproduced by the coupled-channels calculations including the low-lying quadrupole and octupole vibrations in  $^{32}\text{S}$  and  $^{90}\text{Zr}$ . However, the model with the same coupling scheme fails to reproduce the experimental barrier distribution for  $^{32}\text{S}+^{96}\text{Zr}$ . The coupled-channels calculation including the neutron transfer channels in the system  $^{32}\text{S}+^{96}\text{Zr}$  gives an improved description of the experimental data. A comparison of the data on  $^{40}\text{Ca}+^{90,96}\text{Zr}$  shows that the two systems  $^{32}\text{S}$ ,  $^{40}\text{Ca}+^{90}\text{Zr}$  display barrier distributions that are similar to each other, whereas the barrier distributions of  $^{32}\text{S}$ ,  $^{40}\text{Ca}+^{96}\text{Zr}$  are both wider and flatter than the those of  $^{40}\text{Ca}+^{90,96}\text{Zr}$ . The present results strongly indicate that neutron transfer plays an important role in the fusion processes.

DOI: 10.1103/PhysRevC.77.014601

PACS number(s): 25.70.Bc, 25.45.Hi, 25.70.Jj

### I. INTRODUCTION

The role of neutron transfer or neutron flow in the process of heavy-ion fusion is a topic of current interest. Zagrebaev [1] presented a model incorporating neutron transfer in the coupled-channels (CC) approach. He showed that the intermediate neutron transfer channels with positive  $Q$  value really enhance the fusion cross section at sub-barrier energies. Wang *et al.* [2,3] recently developed an improved quantum molecular dynamics (ImQMD) model. By detailed calculations of the ImQMD, they found that a flow of neutron occurs between the projectile and target when they come close together, resulting in a neck. In addition, the neutron flow results in the  $N/Z$  equilibrium between target and projectile nuclei during the collision. Because of the neck formation, the colliding nuclei fuse through the dynamic barrier which is lower than the static barrier. Almost two decades ago, Stelson *et al.* [4–6] came to the same conclusion. They proposed an empirical approach and found that many experimental data can be well described by a flat distribution of barriers with the lower energy cutoff, which corresponds to the energy at which the nuclei come sufficiently close together for neutrons to flow freely between the target and projectile.

On the experimental side, precise fusion excitation functions have been measured for the  $^{40,48}\text{Ca}+^{90,96}\text{Zr}$ ,  $^{40}\text{Ca}+^{94}\text{Zr}$  at near- and sub-barrier energies, and the fusion barrier distributions have been extracted from the measured excitation functions [7–10]. The barrier distributions of  $^{40,48}\text{Ca}+^{90}\text{Zr}$  as well as  $^{48}\text{Ca}+^{96}\text{Zr}$  can be rather reasonably well reproduced by the coupled-channels calculations that take inelastic excitations into account. However, this coupling scheme fails for the reaction systems  $^{40}\text{Ca}+^{94,96}\text{Zr}$ . At sub-barrier energies, these two systems show a large enhancement in the cross sections with respect to the other systems and to the CC calculations including the couplings to the inelastic

excitations only. These results indicate that couplings to neutron transfer channels may play a role in the sub-barrier fusion of  $^{40}\text{Ca}+^{94,96}\text{Zr}$ .

It has been proposed [11,12] theoretically that information on the distribution of potential barriers may be extracted from the scattering excitation function at backward angles. Based on the relationship between transmission coefficient and reflection coefficient, we have confirmed experimentally [13] that except for some details, the barrier distributions extracted from quasi-elastic scattering and from the fusion excitation function are the same. Therefore, precise measurements of elastic and/or quasi-elastic excitation functions may provide another way of deriving barrier distributions. In the present work, we have measured with high precision the quasi-elastic scattering of  $^{32}\text{S}+^{90,96}\text{Zr}$  around the Coulomb barrier at backward angles and extracted the barrier distributions from the excitation functions of quasi-elastic scattering. Our present results may provide further evidence for the effects of neutron transfer with positive  $Q$  value on the sub-barrier fusion reactions.

### II. EXPERIMENT AND RESULTS

The experiment was carried out with a collimated  $^{32}\text{S}$  beam from the HI-13 tandem accelerator at CIAE, Beijing. The targets were evaporations of  $^{90}\text{ZrO}_2$  ( $100\ \mu\text{g}/\text{cm}^2$ ) and  $^{96}\text{Zr}_2\text{O}_3$  ( $140\ \mu\text{g}/\text{cm}^2$ ) on carbon backings of  $20\ \mu\text{g}/\text{cm}^2$  in thickness. The target isotopic enrichments were 99.4% and 95.6% for  $^{90}\text{Zr}$  and  $^{96}\text{Zr}$ , respectively. Two Si(Au) detectors, located at  $\pm 20^\circ$  with respect to the beam direction, were used to monitor the Rutherford scattering, i.e., the counting ratio of the two monitors allowed us to keep watch on any horizontal offset of the beam position, and the counts of the Rutherford events detected by the monitors were used to normalize the cross section measurements. Five sets of  $\Delta E$ - $E$  telescopes and two sets of Si(Au) detectors were set at seven backward angles of  $154.83^\circ$ ,  $158.14^\circ$ ,  $159.07^\circ$ ,  $160.00^\circ$ ,  $160.93^\circ$ ,  $161.86^\circ$ , and  $165.17^\circ$ . The quasi-elastic scattering was measured for

\* martin@ciae.ac.cn

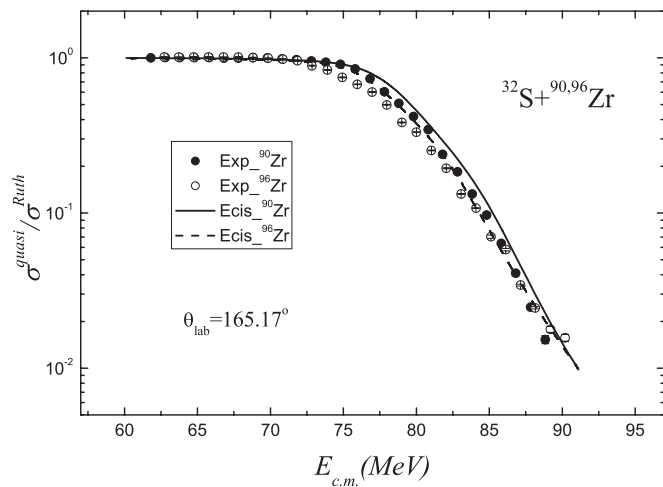


FIG. 1. Ratio of the quasi-elastic scattering differential cross section to the Rutherford scattering cross section at  $165.17^\circ$  as a function of center-of-mass energy for  $^{32}\text{S} + ^{90,96}\text{Zr}$ . The solid and open circles are the experimental data for  $^{32}\text{S} + ^{90}\text{Zr}$  and  $^{32}\text{S} + ^{96}\text{Zr}$ , respectively. The solid and dashed lines represent the ECIS79 calculations for the corresponding reaction systems.

both targets in the laboratory energy range from 84.25 to 120.85 MeV with an energy step  $\Delta E = 0.36$  MeV. Energy loss in targets was considered in our data analysis. Apart from the carbon backing, the average beam energy losses in the targets were  $\delta E = 440\text{--}490$  and  $580\text{--}640$  keV, depending on the beam energy, for  $^{90}\text{Zr}$  and  $^{96}\text{Zr}$ , respectively. The cross sections of quasi-elastic scattering were normalized with the counts of elastic scattering in the two monitors. The experimental error includes the statistic error of the event counts only. The relative error of the cross sections is less than 1% at low energies and about 3% at high energies. A typical example of the excitation functions of quasi-elastic scattering measured at  $165.17^\circ$  is shown in Fig. 1. In the figure, the solid and dashed lines illustrate the CC calculations with ECIS79 code for  $^{32}\text{S} + ^{90}\text{Zr}$  and  $^{32}\text{S} + ^{96}\text{Zr}$ , respectively. The inelastic scattering from two lowest  $2^+$  and  $3^-$  excitation states in  $^{90}\text{Zr}$  ( $\beta_2 = 0.09$ ,  $\beta_3 = 0.22$ ) and  $^{96}\text{Zr}$  ( $\beta_2 = 0.08$ ,  $\beta_3 = 0.27$ ) were included in the calculated differential cross section.

The barrier distribution can be deduced from quasi-elastic scattering excitation function [14] as follows:

$$D^{\text{qel}}(E) = -\frac{d}{dE} \left( \frac{d\sigma^{\text{qel}}}{d\sigma^R}(E) \right), \quad (1)$$

where  $d\sigma^{\text{qel}}$  and  $d\sigma^R$  are the quasi-elastic scattering and the Rutherford scattering differential cross sections, respectively. Theoretically,  $d\sigma^{\text{qel}}$  and  $d\sigma^R$  should be the differential cross sections at  $\theta = 180^\circ$ . However, it is impossible experimentally to detect scattering particles at  $\theta = 180^\circ$ . So instead, the detectors were set up at backward angles as close to  $180^\circ$  as possible. Correspondingly, when barrier distributions are deduced, the center-of-mass energy  $E$  should be reduced by the centrifugal energy  $E_{\text{cent}}$ , with

$$E_{\text{cent}} = E \frac{\text{cosec}(\theta_{\text{c.m.}}/2) - 1}{\text{cosec}(\theta_{\text{c.m.}}/2) + 1}, \quad (2)$$

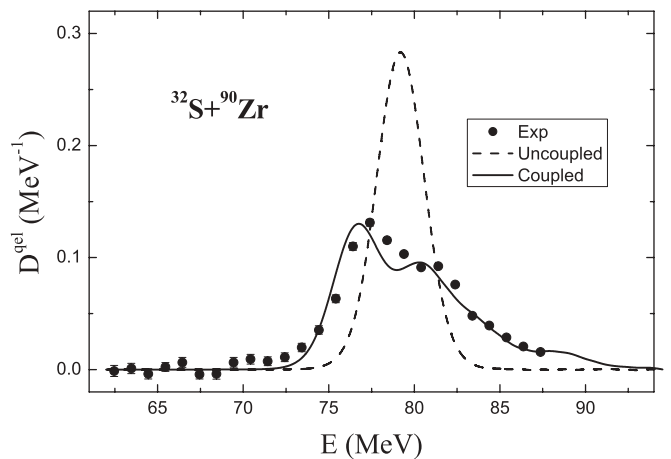


FIG. 2. Barrier distribution for  $^{32}\text{S} + ^{90}\text{Zr}$  deduced from the excitation function of quasi-elastic scattering at backward angle. The dashed and solid lines represent the uncoupled calculation and the CC calculation without neutron transfer, see text for details.

where  $\theta_{\text{c.m.}}$  is the angle in the center-of-mass system. With Eq. (1), the barrier distributions for  $^{32}\text{S} + ^{90,96}\text{Zr}$  were deduced from the excitation functions of quasi-elastic scattering at backward angles; they are displayed as solid circles with error bars in Figs. 2 and 3. The relative error of the data for the barrier distributions is between 1% and 7%. The error bars in the figures are a little larger or less than the size of data point. The barrier distributions obtained at different backward angles are basically same. The lines in Figs. 2 and 3 are the results of the CC calculations with and without coupling, which will be discussed below in detail.

### III. COUPLED-CHANNELS CALCULATIONS

Coupled-channels calculations have been performed with the CCDEF code. Table I lists the experimental information on the low-lying collective excitations in  $^{32}\text{S}$  and  $^{90,96}\text{Zr}$ , which were included in the coupling scheme. From the calculated fusion excitation functions, the barrier distributions of  $^{32}\text{S} + ^{90,96}\text{Zr}$  were deduced, and they are compared with experimental data in Figs. 2 and 3. It may be seen that the experimental barrier distribution of  $^{32}\text{S} + ^{90}\text{Zr}$  is well reproduced by the CC calculation with the couplings to the low-lying quadrupole and octupole vibrations in  $^{32}\text{S}$  and  $^{90}\text{Zr}$ .

TABLE I. Excitation energies  $E_x$ , spin and parities  $\lambda^\pi$ , and deformation parameters  $\beta_\lambda$  for  $^{32}\text{S}$  and  $^{90,96}\text{Zr}$ .

Nucleus	$E_x$ (MeV)	$\lambda^\pi$	$\beta_\lambda$
$^{32}\text{S}$	2.230	$2^+$	0.32
	5.006	$3^-$	0.40
$^{90}\text{Zr}$	2.186	$2^+$	0.09
	2.748	$3^-$	0.22
$^{96}\text{Zr}$	1.751	$2^+$	0.08
	1.897	$3^-$	0.27

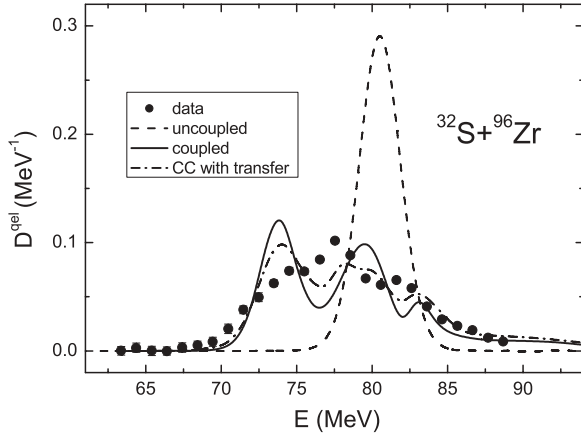


FIG. 3. Same as Fig. 2, but for  $^{32}\text{S}+^{96}\text{Zr}$ . The dash-dotted line represents the CC calculations in which the neutron transfer channels were taken into account.

The distribution of  $^{32}\text{S}+^{90}\text{Zr}$  has two peaks at about 77 and 82 MeV. The theoretical calculation reappears these peaks although at slightly lower energies. Moreover, the low-energy side of the distribution is also satisfactorily reproduced by the CC calculation.

However, the CC calculation with the same coupling scheme fails for the reaction system  $^{32}\text{S}+^{96}\text{Zr}$ . The experimental barrier distribution of  $^{32}\text{S}+^{96}\text{Zr}$  shows that it has a three-peak structure, i.e., a peak or a shoulder, a main peak, and a weak peak at about 74, 77.5, and 82 MeV, respectively. This structure is not reproduced properly by the CC calculation with the couplings to the low-lying quadrupole and octupole vibrations in  $^{32}\text{S}$  and  $^{96}\text{Zr}$ . The calculated barrier distribution shows a more clear peak structure than that of the experimental barrier distribution. The obscurity of the structure in the experimental barrier distribution may arise from the surface nature of the quasi-elastic collision. To get a detailed structure of the distribution, it is highly required that one perform precise measurement of the fusion excitation function for the reaction system  $^{32}\text{S}+^{96}\text{Zr}$ . Apart from the difference mentioned above, the peak positions are not exactly the same, and the intensity of the peaks between the calculated and experimental barriers are different. Contrary to the experimental result, the calculated barrier distribution has more weight in the low-energy peak than that of the middle one. In addition, it is worth noting that the experimental barrier distribution of  $^{32}\text{S}+^{96}\text{Zr}$  is flatter and extends to lower energies than does the barrier distribution of  $^{32}\text{S}+^{90}\text{Zr}$ . Flat distribution with a low-energy tail is thought to be a hint of the existence of

neutron transfer or flow in the fusion processes as suggested by Stelson *et al.* [4–6].

According to the approach of Zagrebaev [1], neutron transfer can be incorporated in the CC calculation with the following penetration probability:

$$T(E, l) = \int f(B) \frac{1}{N_{\text{tr}}} \sum_{\kappa} \int_{-E}^{Q_0(\kappa)} \alpha_{\kappa}(E, l, Q) \times P_{\text{HW}}(B; E + Q, l) dQ dB, \quad (3)$$

where  $f(B)$  is the normalized barrier distribution,  $Q_0(\kappa)$  is the  $Q$  value for the ground-state to ground-state transfer of the  $\kappa$ th neutron,  $P_{\text{HW}}$  is the usual Hill-Wheeler formula [15] of the quantum penetration probability,  $\alpha_{\kappa}(E, l, Q)$  is the probability for the transfer of  $k$  neutrons at the center-of-mass energy  $E$  and relative motion angular momentum  $l$  in the entrance channel to the final state with  $Q \leq Q_0(k)$ , and  $N_{\text{tr}}$  is the normalization constant for the transfer probability.

The  $Q$  values for ground-state to ground-state neutron pickup transfer channels of  $^{32}\text{S}+^{90,96}\text{Zr}$  are listed in Table II. For  $^{32}\text{S}+^{90}\text{Zr}$ , since all ground-state  $Q$  values are negative, neutron transfer channels, as expected, should not play any important role in the dynamics of sub-barrier fusion. On the other hand, the ground-state  $Q$  values of neutron pickup from  $1n$  up to  $6n$  channels are all positive for  $^{32}\text{S}+^{96}\text{Zr}$ . It means that in its intermediate channels, the systems between  $^{33}\text{S}+^{95}\text{Zr}$  and  $^{38}\text{S}+^{90}\text{Zr}$  will experience a gain in energy due to the neutron flow, which may increase the penetration probability of the Coulomb barrier and lead to a noticeable increase in the fusion cross section at sub-barrier energies. To take the effects of neutron transfer on fusion reaction into account, we performed the CC calculation using the approach of Zagrebaev [1], i.e., Eq. (3). In this CC calculation, couplings to six neutron transfer channels as well as to the low-lying quadrupole and octupole vibrations in  $^{32}\text{S}$  and  $^{96}\text{Zr}$  were included. The relevant coupling parameters are listed in Tables I and II. The extracted barrier distribution from this CC calculation (shown in Fig. 3 as a dash-dotted line) is flatter than that from the CC calculation without neutron transfer channels coupling and gives a somewhat better description of the experimental data.

$^{40}\text{Ca}+^{96}\text{Zr}$  is an ideal reaction system for probing the effects of neutron transfer on sub-barrier fusion [7]. Therefore, it is worth comparing the barrier distributions of  $^{32}\text{S}+^{90,96}\text{Zr}$  with those of  $^{40}\text{Ca}+^{90,96}\text{Zr}$  as show in Fig. 4. One notices that except for a third peak in high-energy region in the  $^{40}\text{Ca}+^{90}\text{Zr}$  case, the two systems  $^{32}\text{S}$ ,  $^{40}\text{Ca}+^{90}\text{Zr}$  display similar barrier distributions. While the barrier distributions of  $^{32}\text{S}$ ,  $^{40}\text{Ca}+^{96}\text{Zr}$

TABLE II.  $Q$  values (MeV) for ground-state to ground-state neutron pickup transfer channels for the  $^{32}\text{S}$ ,  $^{40}\text{Ca}+^{90,96}\text{Zr}$  systems.

System	+1n	+2n	+3n	+4n	+5n	+6n
$^{32}\text{S}+^{90}\text{Zr}$	-3.33	-1.229	-6.59	-6.319	-14.689	-16.429
$^{32}\text{S}+^{96}\text{Zr}$	0.788	5.737	4.508	7.655	3.332	4.168
$^{40}\text{Ca}+^{90}\text{Zr}$	-3.608	-1.438	-5.858	-4.336	-9.602	-8.980
$^{40}\text{Ca}+^{96}\text{Zr}$	0.510	5.528	5.240	9.638	8.419	11.617

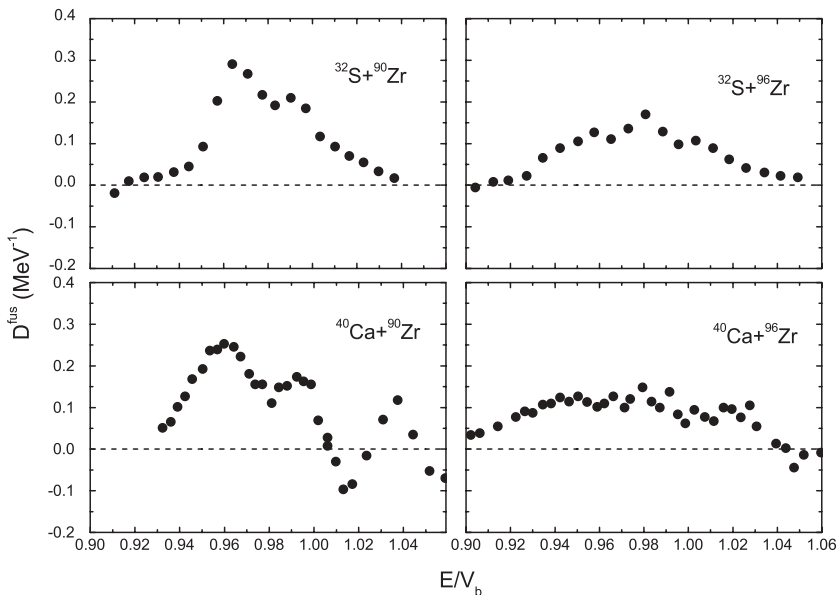


FIG. 4. Comparison of the barrier distributions for the systems  $^{32}\text{S}+^{90,96}\text{Zr}$  and  $^{40}\text{Ca}+^{90,96}\text{Zr}$ .

are flatter and extend to lower energies than those of  $^{32}\text{S}$ ,  $^{40}\text{Ca}+^{90}\text{Zr}$ . By inspection of Table II, one will immediately find that the ground-state  $Q$  values of neutron pickup from  $1n$  up to  $6n$  channels are all positive for  $^{32}\text{S}$ ,  $^{40}\text{Ca}+^{96}\text{Zr}$ , but all negative for the two reaction systems with  $^{90}\text{Zr}$  target.

#### IV. SUMMARY

The differential cross sections of quasi-elastic scattering at backward angles were measured with high precision for  $^{32}\text{S}+^{90,96}\text{Zr}$  around the Coulomb barrier. From the precise measured excitation functions, barrier distributions were extracted as the differential of  $d\sigma^{\text{qel}}/d\sigma^R$  with respect to  $E$ . The data have been analyzed in terms of the coupled-channels model with the CCDEF code. Good agreement between experiment and theory is found for  $^{32}\text{S}+^{90}\text{Zr}$  by including the couplings to the low-lying quadruple and octupole vibrations in  $^{32}\text{S}$  and  $^{90}\text{Zr}$ . However, the CC calculation with the same coupling scheme fails to reproduce the experimental barrier distribution for  $^{32}\text{S}+^{96}\text{Zr}$ , which is flatter and wider than that for  $^{32}\text{S}+^{90}\text{Zr}$ . Therefore, for the system  $^{32}\text{S}+^{96}\text{Zr}$ , the CC calculation including six neutron transfer channels as well as the low-lying quadruple and octupole vibrations in  $^{32}\text{S}$  and  $^{96}\text{Zr}$  were performed. Although the result of the CC calculation including the neutron transfer channels give a somewhat better description of the experimental data, the agreement is not satisfactory. The theoretical distribution shows a more obvious peaklike structure than the experimental one. Besides, the calculated intensities of the peaks are at

variance with those of the experimental distribution. It seems to us that to investigate the detailed structure of the barrier distribution, precise measurement of the fusion excitation function for  $^{32}\text{S}+^{96}\text{Zr}$  are highly required. In addition to the fusion excitation function, the neutron transfer cross section measurements for this system should provide useful information on the coupling strength of neutron transfer. We believe that the combined CC calculations including both the fusion and transfer channels will bring about a deeper understanding of the role of neutron transfer on the fusion process.

The comparison of the data on  $^{40}\text{Ca}+^{90,96}\text{Zr}$  shows that the two systems  $^{32}\text{S}$ ,  $^{40}\text{Ca}+^{90}\text{Zr}$  display similar barrier distributions. However, the barrier distributions of  $^{32}\text{S}$ ,  $^{40}\text{Ca}+^{96}\text{Zr}$  are wider and flatter than those of  $^{32}\text{S}$ ,  $^{40}\text{Ca}+^{90}\text{Zr}$ . The obviously different behaviors of these reaction systems strongly indicate that neutron transfer plays an important role in the fusion process, as does the fact that the ground-state  $Q$  values of neutron pickup from  $1n$  up to  $6n$  channels are all positive for  $^{32}\text{S}$ ,  $^{40}\text{Ca}+^{96}\text{Zr}$ , but all negative for the two reaction systems with  $^{90}\text{Zr}$  target.

#### ACKNOWLEDGMENTS

This work was partially supported by the National Natural Science Foundation of China under Grants Nos. 10275095, 10575134, 10575134, 10675169 and the Major State Basic Research Developing Program No. 2007CB815000.

- [1] V. I. Zagrebaev, Phys. Rev. C **67**, 061601(R) (2003).  
 [2] N. Wang, Z. X. Li, and X. Z. Wu, Phys. Rev. C **65**, 064608 (2002).  
 [3] N. Wang, Z. Li, X. Wu, J. Tian, Y. X. Zhang, and M. Liu, Phys. Rev. C **69**, 034608 (2004).

- [4] P. H. Stelson, Phys. Lett. **B205**, 190 (1988).  
 [5] P. H. Stelson, H. J. Kim, M. Beckerman, D. Shapira, and R. L. Robinson, Phys. Rev. C **41**, 1584 (1990).  
 [6] W. Rowley, G. R. Satchler, and P. H. Stelson, Phys. Lett. **B254**, 21 (1991).

- [7] H. Timmers, D. Ackermann, S. Beghini, L. Corradi, J. H. He, G. Montagnoli, F. Scarlassara, A. M. Stefanini, and N. Rowley, Nucl. Phys. **A633**, 421 (1998).
- [8] H. Q. Zhang, Z. H. Liu, F. Yang, C. J. Lin, M. Ruan, Y. W. Wu, Z. X. Li, X. Z. Wu, K. Zhao, and N. Wang, Chin. Phys. Lett. **22**, 3048 (2005).
- [9] A. M. Stefanini, F. Scarlassara, S. Beghini, G. Montagnoli, R. Silvestri, M. Trotta, B. R. Behera, L. Corradi, E. Fioretto, A. Gadea, Y. W. Wu, S. Szilner, H. Q. Zhang, Z. H. Liu, M. Ruan, F. Yang, and N. Rowley, Phys. Rev. C **73**, 034606 (2006).
- [10] A. M. Stefanini, B. R. Behera, S. Beghini, L. Corradi, E. Fioretto, A. Gadea, G. Montagnoli, N. Rowley, F. Scarlassara, S. Szilner, and M. Trotta, Phys. Rev. C **76**, 014610 (2007).
- [11] A. T. Kruppa, P. Romain, M. A. Nagarajan, and N. Rowley, Nucl. Phys. **A560**, 845 (1993).
- [12] M. V. Andres, N. Rowley, and M. A. Nagarajan, Phys. Lett. **B202**, 292 (1988).
- [13] H. Q. Zhang, F. Yang, C. J. Lin, Z. H. Liu, and Y. M. Hu, Phys. Rev. C **57**, R1047 (1998).
- [14] H. Timmer, J. R. Leigh, M. Dasgupta, D. J. Hinde, R. C. Lemmon, J. C. Mein, C. R. Morton, J. O. Newton, and N. Rowley, Nucl. Phys. **A584**, 190 (1995).
- [15] D. L. Hill and J. A. Wheeler, Phys. Rev. **89**, 1102 (1953).